ACS APPLIED MATERIALS & INTERFACES

Research Article

www.acsami.org

NiO/MAPbI$_{3-x}$Cl$_x$/PCBM: A Model Case for an Improved Understanding of Inverted Mesoscopic Solar Cells

Vanira Trifiletti,[†] Vittoria Roiati,[†,‡] Silvia Colella,[§] Roberto Giannuzzi,[†] Luisa De Marco,[†] Aurora Rizzo,[†,§] Michele Manca,[†] Andrea Listorti,*[,†,§] and Giuseppe Gigli[†,§,#]

[†]Center for Bio-Molecular Nanotechnology - Fondazione Istituto Italiano di Tecnologia, Via Barsanti, 73010 Arnesano, Lecce, Italy

[‡]Department of Physics, Politecnico di Milano, p.zza Leonardo da Vinci 32, 20133 Milano, Milano, Italy

[§]NNL – National Nanotechnology Laboratory, CNR Istituto Nanoscienze, Distretto Tecnologico, Via Arnesano 16, 73100 Lecce, Lecce, Italy

[#]Dipartimento di Matematica e Fisica "E. De Giorgi", Università del Salento, Via per Arnesano, 73100 Lecce, Lecce, Italy

Supporting Information

ABSTRACT: A spectroscopic investigation focusing on the charge generation and transport in inverted p-type perovskite-based mesoscopic (Ms) solar cells is provided in this report. Nanocrystalline nickel oxide and PCBM are employed respectively as hole transporting scaffold and hole blocking layer to sandwich a perovskite light harvester. An efficient hole transfer process from perovskite to nickel oxide is assessed, through time-resolved photoluminescence and photoinduced absorption analyses, for both the employed absorbing species, namely MAPbI$_{3-x}$Cl$_x$ and MAPbI$_3$. A striking relevant difference between p-type and n-type perovskite-based solar cells emerges from the study.

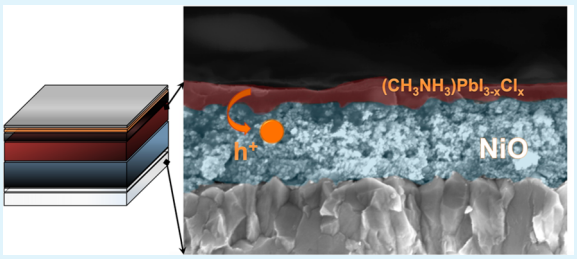

KEYWORDS: *perovskite, solar cells, NiO, charge transfer and transport*

INTRODUCTION

Hybrid organic–inorganic perovskites have emerged at the forefront of the most exciting and innovative materials for photovoltaic (PV) applications, delivering ground-breaking efficiency and holding the promise of accessible scalability with low-cost solution processability, for an abundant and sustainable energy supply.[1−5] Organometal halide perovskites possess intense and broad light absorption, remarkable ambipolar charge mobility, and very low nonradiative carrier recombination rates leading to impressive charge diffusion length.[6−9] These fascinating properties allow the inclusion of this material in a variety of device architectures exploring different manufacture procedures, targeting diverse potential applications, and achieving outstanding PV performances, above 19%.[10−14] Emerged as an evolutionary step of solid state sensitized solar cells (ss-SSC), in most of the explored and more performing perovskite-based PV device architectures (PSCs), the electrons are collected at the transparent conductive oxide (TCO) thin film and the holes migrate at the evaporated metal contacts in a so-called n-type device configuration.[1] TiO_2 and 2,2′,7,7′-tetrakis(*N*,*N*-di-4-methoxyphenylamino)-9,9′-spirobifluorene (spiro-OMeTAD) are the most employed charge extracting materials of such device configuration, in virtue of their good optical transparency and ideal band alignment with respect to halide perovskites.[15] Nonetheless, many groups attempt using alternative charge selective materials with higher conductivity or easy processability, such as TiO_2/graphene composite,[16] ZnO,[17] and as hole transport materials poly[bis(4-phenyl)(2,4,6-trimethylphenyl)-amine] (PTAA),[18] tetrathiafulvalene derivative,[19] and CuSCN.[20] An alternative explorative path foresees a variation of the fundamental device architecture. Inverted PSCs with reverse current flow direction (photoinduced holes instead of electrons collected though the front conductive glass substrate) allow, in fact, the evaluation of additional extracting materials, such as PEDOT:PSS, NiO, and phenyl-C61-butyric acid methyl ester (PCBM), classically employed in organic PV (OPVs).[21−23] Withstanding the high performances of devices embedding PEDOT:PSS as hole transporter, it is known that this material could be critical for device lifetime. Its hygroscopic nature allows in fact absorption of water, which facilitates etching of the ITO layer and decomposition of perovskite.[24] Foreseeing the obtainment of a stable and long living device, the use of inorganic conductors for both electron and hole transport layers might be ideal to protect the moisture-sensitive perovskite absorber better than organic materials. Furthermore, inorganic mesostructured (Ms) scaffold allows a better control of the perovskite layer and confers to the material more suitable properties for the application in PSCs.[3] In this vision, NiO represents one of the best candidates as hole extracting layer in

Received: December 9, 2014
Accepted: February 3, 2015
Published: February 3, 2015

DOI: 10.1021/am508678p
ACS Appl. Mater. Interfaces 2015, 7, 4283−4289

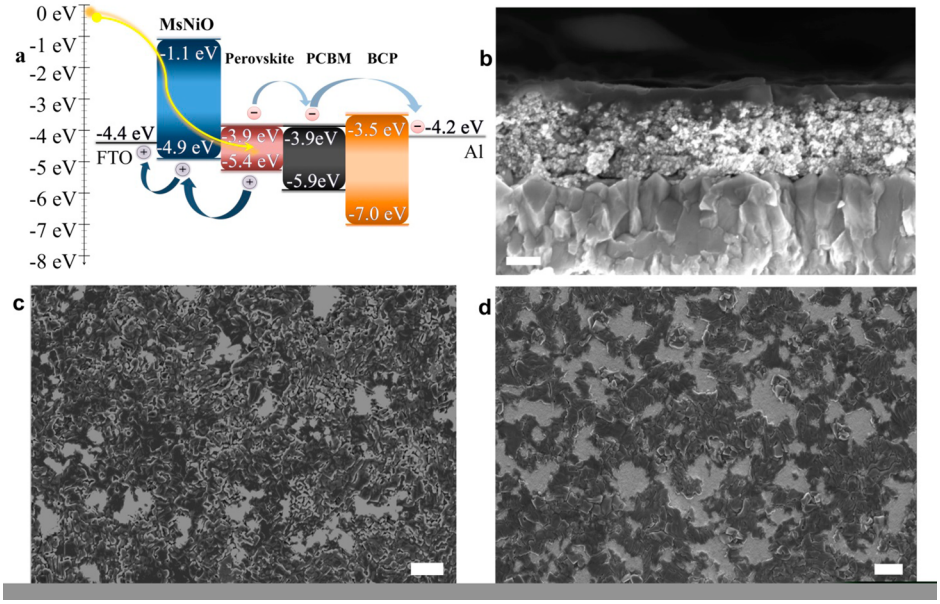

Figure 1. (a) A sketch of the inverted p-type solar cell architecture integrated with a band energy diagram for its constituents and (b) the corresponding cross-section SEM image (scale bar 200 nm). Plane view SEM inspection of (c) $MAPbI_3$ and (d) $MAPbI_{3-x}Cl_x$ spin-coated onto NiO film in a one-step fashion (scale bar 2 μm).

an inverted architecture considering the excellent optical, electrical, and thermal properties that would confer to the final device.

In addition, the exploration of different materials and diverse cell configurations is of fundamental importance for a full elucidation of the PSCs PV conversion mechanism. Taking advantage of these efforts, few alternative basic descriptions of perovskite-based solar cells working principles have been paved out.[6−8,25−32] Withstanding these research steps forward, many questions, above all J/V hysteresis behavior, are far from being rationalized and interfere as significant drawbacks with the technological declination of this emerging technology.[3,33,34] The purpose of the present work is to assess the fundamental charge transfer/transport mechanisms regulating the photovoltaic behavior of both $MAPbI_{3-x}Cl_x$- and $MAPbI_3$-based (MA = CH_3NH_3) inverted solar cells employing NiO as p-type Ms scaffold, with the aim of highlighting the differences between this architecture and the majorly investigated n-type one. A rationalization of the working mechanism will allow an intelligent design of this class of device aiming at improve their processability and performances. As our study is dedicated to the fundamental understanding of device working principles with no aspiration of obtaining high PV efficiencies we focus on the one-step solution process, to keep comparable deposition conditions between two light harvesting materials. Furthermore, to the best of our knowledge, an investigation of the photoinduced charge transfer in mixed-halide-perovskites/NiO systems has not been reported so far.

RESULTS AND DISCUSSION

We realize one-step solution processed perovskite sensitized solar cells (**PSSC**) inverted devices onto Ms p-type NiO oxide with either $MAPbI_3$ or mixed halide $MAPbI_{3-x}Cl_x$ hybrid perovskites as absorber. A thin spin-coated PCBM electron transporting layer (40 nm), a 10 nm thick thermally evaporated bathocuproine (BCP) hole blocking layer and aluminum back contact complete the device stack (Figure 1a). The details of the experimental methods are described in the Supporting Information.

SEM cross-section image of the $MAPbI_{3-x}Cl_x$ based p-type device is reported in Figure 1b. The MsNiO scaffold (≈400 nm), whose properties were assessed via optical, morphological, and electrical characterization reported in the Supporting Information (S1−3) shows sensible transparency, spanning from a few % to 15% decrease in light transmittance in the visible region of the spectrum. The intrinsic competitive absorption, as well as its rather low hole mobility (10^{-5} to 10^{-3} $cm^2\ V^{-1}\ s^{-1}$), have been widely proved in p-type sensitized solar cells and largely hinder the achievement of high J_{sc} and *FF* in those devices.[22,35,36]

Both $MAPbI_3$ and $MAPbI_{3-x}Cl_x$ perovskites have been processed through the same procedure. Despite the high solubility of PbI_2 allowing the development of several deposition techniques to achieve smooth $MAPbI_3$ films on NiO,[10,36−38] the poor solubility of $PbCl_2$ importantly limits the possibilities of optimization for mixed halide $MAPbI_{3-x}Cl_x$ perovskite. For this reason in our comparative study $MAPbI_{3-x}Cl_x$ and $MAPbI_3$ are both spin-coated in one-step from the precursor solution of either $PbCl_2$ or PbI_2 with MA in dimethylformamide (DMF). As expected, SEM imaging (Figure 1) shows that the coverage and morphology of the two perovskites onto NiO are similar. It is worth noticing that, differently for n-type architectures, a flat perovskite film is essential to obtain high performing p-type solar cells; indeed PCBM, due to its low conductivity, must be deposited as a very thin film. About 55 nm has been proven to be the ideal thickness in the PEDOT:PSS/$MAPbI_3$/PCBM configuration,[23] where the film only partially fills the voids of the perovskite underlayer, as shown in Figure S4. Figure 2 shows the current−voltage (J−V) characteristics in dark and under illumination of both $MAPbI_{3-x}Cl_x$ (red lines) and $MAPbI_3$ (black lines) p-type solar cells. From the J−V curve measured under standard AM1.5G conditions, the J_{sc}, V_{oc}, fill factor, and power conversion efficiency (PCE) are determined as 5.7 mA/cm^2, 0.89 V, 0.56, 2.9% and 6.8 mA/cm^2, 0.81 V, 0.49, 2.7% for the

DOI: 10.1021/am508678p
ACS Appl. Mater. Interfaces 2015, 7, 4283−4289

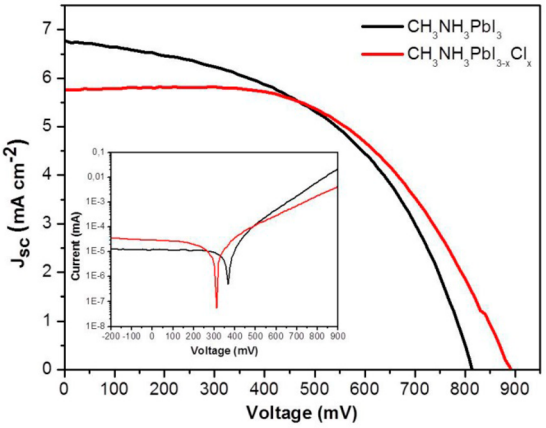

Figure 2. J–V characteristics measured under 100 mW cm^2 AM1.5G illumination for $MAPbI_{3-x}Cl_x$ (red line) and $MAPbI_3$ (black line) in an inverted p-type geometry with mesoporous NiO. Inset: Corresponding J–V characteristics in dark.

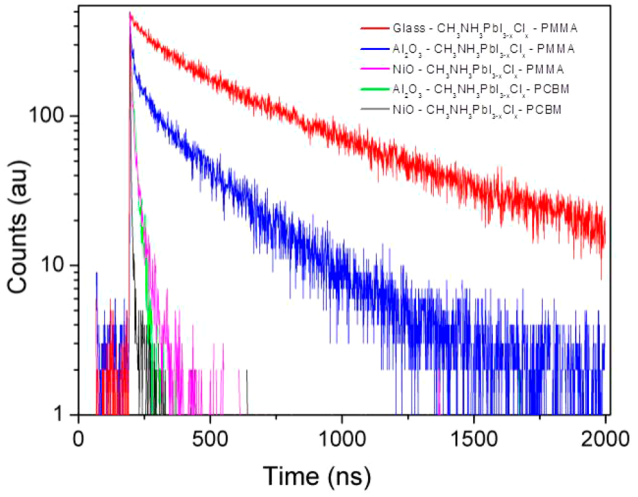

Figure 3. Time correlates single photon counting analysis of samples aimed to decouple the device interfaces from each other: Perovskite ($MAPbI_{3-x}Cl_x$ = PERO) between inert materials (Glass and PMMA or Al_2O_3 and PMMA), deposited on p-type conductive oxide (NiO/$MAPbI_{3-x}Cl_x$/PMMA) and with extracting electron layer on top (NiO/$MAPbI_{3-x}Cl_x$/PCBM and Al_2O_3/$MAPbI_{3-x}Cl_x$/PCBM). λ_{exc}: 635 nm λ_{em} = 760 nm.

$MAPbI_{3-x}Cl_x$ and $MAPbI_3$, respectively. Tests performed at different precursors concentrations are reported in Table S1.

The performances obtained are in line with the device and material preparation procedures. The main limiting factor for the achievement of high photo conversion efficiencies is the deposition of the perovskites in a single step process. This methodology has been proved not to be the best way to boost the performances of NiO/perovskite solar cells.[10,21,23,35−37] In fact, to the best of our knowledge, we obtained the highest PV conversion efficiencies withstanding this material preparation procedure.[21,39] The choice of single step deposition is related to the aim of comparing two different types of perovskite, as this is the only methodology allowing to prepare them using the same protocols. As a result the light harvesting properties for the two absorbers are comparable, as evidenced from the UV–vis absorption reported in Figure S5.

In order to compare the photoinduced processes occurring in our $MAPbI_{3-x}Cl_x$ and $MAPbI_3$ p-type solar cells with the one occurring in classic n-type ones, PL quenching and cw-photoinduced absorption on working device and on derived reference systems are carried out. Perovskite photoluminescence (PL) quenching is investigated when the material is embedded in model samples suited to decouple the various device interfaces. Figure 3 schematizes the results of time correlated single photon counting analysis for bare perovskite ($MAPbI_{3-x}Cl_x$) sandwiched between inert materials (Glass and PMMA) as a reference, and $MAPbI_{3-x}Cl_x$ deposited onto mesoporous substrates (Al_2O_3 and NiO), with or without electron accepting layer (PCBM) on top. It is evident that both electron transporting material (PCBM) and hole transporting substrate (Ms NiO) are efficient PL quencher, giving the first proof of an eventual efficient charge transfer at the interface with perovskite. Caution is needed in this conclusion, since, as already reported,[26,40,41] PL quenching may also be due to morphological and structural reasons, as evidenced by the net PL quenching observed for the Al_2O_3/$MAPbI_{3-x}Cl_x$/PMMA sample, where no charge transfer takes place, compared to the $MAPbI_{3-x}Cl_x$ on glass. Moreover, the influence of the oxide mesoporous scaffold has been discussed in terms of perovskite doping and its influence on charge recombination mechanism and so PL quantum efficiency,[42] but no work has been done on p-type scaffold and further analysis is required on this important topic. Notably in the complete device (NiO/$MAPbI_{3-x}Cl_x$/PCBM) PL is almost totally quenched and as further proved below, charge transfer is certain in this system.

To directly monitor charge extraction in the investigated systems, we performed continuous wavelength (cw) Photo-Induced Absorption (PIA). In cw-PIA, an on/off continuum laser source (square wave modulated by a mechanical chopper) provides the monochromatic excitation, while a white light source probes the presence of photogenerated species at specific wavelengths. Formation and recombination of transient species (such as oxidized dye and charge carriers) are monitored in the long time scale roughly given by the inverse of the chopper frequency (μs-ms time domain). Figure 4a reports the in phase and out of phase photoinduced absorption (cw-PIA) spectrum of a working device embedding perovskite on Ms NiO substrate covered with PCBM electron transporting layer. The signals constitute strong evidence of efficient hole transfer from perovskite to NiO substrate and a qualitative estimation of the process efficiency compared to a known system. Perovskite absorption edge bleaching is clearly recognizable in the in phase channel around 760 nm, together with the broad absorption of NiO^+ after 800 nm. The latter feature is strongly present both in the in phase and out of phase components of the signal, indicating long living charges in the mesoporous matrix. To give an estimation of the amount of the injected charges (given that the signal amplitude is both due to the absorption cross section of the species and their lifetime), Figure 4c reports the same measurement performed on a p-type Dye-sensitized Solar Cell (pDSC) embedding coumarine dye C343 (Sigma-Aldrich).[43] The absorption spectra of the dye and the perovskite are shown in Figure 4b, and the small difference in absorption at 488 nm (excitation wavelength) is normalized in the reported cw-PIA spectra. The photovoltaic performances of the pDSC, employing 3.2 μm NiO and electrolyte solution in 3-methoxypropionitrile (0.1 M I_2 and 0.5 M tetrabutylammonium iodide), reported in Figure S6 reaches photovoltaic conversion efficiency of ≈0.1%, comparable with the performances reported in the literature,[43,44] pointing out, inter alia, the high quality of the employed nickel oxide. The spectrum in

DOI: 10.1021/am508678p
ACS Appl. Mater. Interfaces 2015, 7, 4283−4289

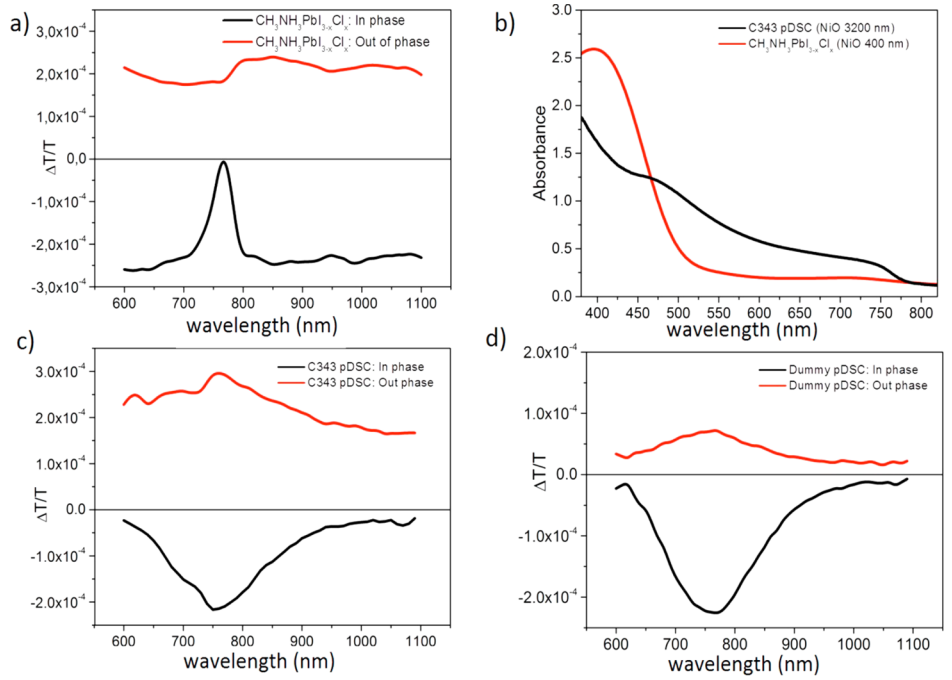

Figure 4. cw-PIA measurements on p-type perovskite device and p-type liquid dye sensitized solar cell obtained with 488 nm excitation and 230 Hz frequency. (a) in phase and out of phase PIA signals obtained for a complete NiO/$MAPbI_{3-x}Cl_x$/PCBM working cell; (b) absorption spectra of liquid pDSC embedding coumarine C343 dye and perovskite cell; (c) in phase and out of phase PIA signals obtained for coumarine DSC working cell; (d) in phase and out of phase PIA signals obtained for a dummy pDSC cell with no dye.

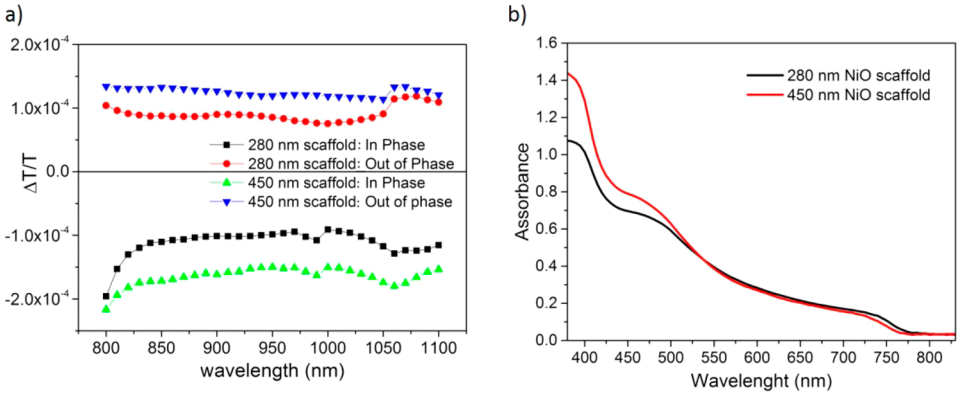

Figure 5. (a) In phase and out of phase cw-PIA signals obtained with the same setup as Figure 4 for two p-type perovskite devices holding different NiO scaffold thickness, 280 nm (red dots and black square) and 450 nm (blue and green triangles); (b) absorption spectra of the two devices.

Figure 4c shows two main features: in the in phase channel the broad absorption of the I_2^- redox intermediate (750 nm)[45] and in the out of phase the absorption of NiO^+ species due to hole injection in the oxide matrix. The electrolyte signal is also reported and isolated in a dummy cell (no dye) with the same architecture in Figure 4d. Oxidized NiO feature and its long living nature, compared to the I_2^- intermediate, has been reported and characterized in several reports.[44,46] The amplitude of the NiO^+ absorption is the very same for the liquid DSC and the perovskite-based device, proving that injection is efficiently happening in the solid state device, and so PL quenching can be attributed to a charge transfer mechanism at the interface.

We have recently demonstrated[26] that electron percolation to the TiO_2 compact layer contact in $MsTiO_2$/perovskite devices is mediated by two different paths: through the titania matrix after injection and majorly through the perovskite itself. Inverted devices have been only minimally spectroscopically investigated, and the photoinduced processes there occurring have been poorly discussed. In this work an efficient charge injection on NiO is verified, similar for the two compounds, orders of magnitude higher than the injection on TiO_2. This result is a crucial difference between inverted perovskite cells and their n-type counterparts; in fact in the present case injection seems to be the dominant mechanism.

In addition, the influence of mesoporous scaffold thickness on cw-PIA signals is investigated comparing 280 and 450 nm thick NiO substrates with the same perovskite concentration (Figure 5a), whose absorption spectra are reported in Figure 5b. The sample with thinner Ms NiO holds a small amount of perovskite flat overstanding layer, giving the sample a smoother morphology compared to the 450 nm one, which presents an almost complete perovskite infiltration in the scaffold. The overstanding layer probably helps charge extraction, as the best

DOI: 10.1021/am508678p
ACS Appl. Mater. Interfaces 2015, 7, 4283−4289

performances are obtained for the thin Ms layer (see devices performances for different Ms NiO thickness in Table S1), and prevents direct connection between the electron conductor and the p-type semiconductor oxide. However, Figure 5a shows how the signal attributed to NiO^+ in a cw-PIA experiment, similar to the one discussed in Figure 4, increases with increasing scaffold thickness. Also the $PCBM^-$ signal around 1050 nm is clearly visible in this enlarged portion of the spectrum.[47] This result demonstrates, again, an efficient charge separation at both interfaces and long living separated charges in the two p and n-type media embedding the perovskite matrix.

cw-PIA spectra obtained on $MAPbI_3$-based devices are reported in Figure S7; those do not differ from what was observed for $MAPbI_{3-x}Cl_x$-based ones suggesting a similar working mechanism for the two perovskites in p-type configuration.

It is interesting to point out here the different roles played by the mesoporous scaffold in n- or p-type architecture: various reports have been investigating cells photovoltaic performances as a function of Ms TiO_2 or Al_2O_3 thickness,[14,48] and morphological conclusions have been drawn correlated to the final device quality. Carefully optimized TiO_2 and Al_2O_3 scaffold seem to have the same role in favoring the formation of more uniform perovskite films, compared to the flat devices, increasing charge collection and minimizing recombination also by reducing the size of perovskite crystals. In other words, apart from a doping effect, n-type scaffolds have a fundamental structural influence, being the charge transport occurring in the perovskite film. The thickness of such a scaffold, comprised in the limits of charge diffusion length characterizing hybrid halide perovskite, is not a limitation to the device performances, apart from optimized morphological considerations. In p-type devices, instead, injection has a crucial role, and the transport mainly occurs in the NiO scaffold. Hole mobility in NiO, as already pointed out, is unimpressive (10^{-5} to 10^{-3} cm^2 V^{-1} s^{-1}), and this could represent a major drawback of the approach. In addition thicker NiO scaffold would absorb more light not destined to the photovoltaic conversion. Figure 5a, where less efficient device, corresponding to the thicker sample, has the higher concentration of free holes in the NiO scaffold, is an eloquent proof of this statement. Therefore, considering the relevance of charge transport, thin scaffold should be employed in a p-type device, potentially guarantying good balance between morphology and transport. Being established an efficient charge injection from mixed halide to NiO, a fundamental issue to be solved toward a further improvement of p-type PSC device is the morphology control of solution processed $MAPbI_{3-x}Cl_x$ and in particular compatibility with the NiO surface.

CONCLUSION

In conclusion, $MAPbI_{3-x}Cl_x$ and $MAPbI_3$ embedded in inverted architectures, employing NiO and PCBM as charge extraction layers, are investigated. Holes injection and transport through NiO mesoporous film is verified to be the dominant mechanism of charge collection, in contrast to what was observed for electrons in mesoporous n-type TiO_2-based devices. Consequently, efforts to achieve efficient perovskite p-type solar cells, based on NiO hole acceptor media, should be devoted to reduction of the NiO thickness and to the optimization of the NiO/perovskite interface. Possible solutions could be the implementation of specific mixed halide perovskite deposition techniques to obtain very smooth and uniform films, such as the double-step deposition or the employment of orthogonal solvents, which would allow a smooth coverage of a thin compact NiO substrate. Alternatively the beneficial effect of the mesostructured scaffold could be kept attempting to employ an inert scaffold such as Al_2O_3 on a thin NiO charge selective layer. Noticeably the latter approach has been followed leading to outstanding PV performance in a report published during the revision process of our manuscript.[49] A fine optimization and engineering of NiO-based solar cells, passing through the comprehension of their basic PV mechanism, would lead in the future to high efficient devices, combined with high voltages and long-term stability.

ASSOCIATED CONTENT

Supporting Information

Experimental section (Morphological, structural, and optical characterization, Electrochemical characterization, Inverted Mesoscopic Solar Cell fabrication and characterization, Dye-sensitized Solar Cell fabrication, Photophysical Characterization), NiO characterization (Transmission spectra of NiO films, FE-SEM image of NiO film deposited on FTO-coated substrates, Plot of $(\alpha h\nu)^2$ against $h\nu$ of the NiO films, Mott–Schottky plots, and Cyclic voltammetry measurements of a NiO thin film), FE-SEM images of PCBM coverage of $MAPbI_{3-x}Cl_x$, Table of photovoltaic parameters of best performing $MAPbI_{3-x}Cl_x$ devices (varying the perovskite concentration in DMF solution and the NiO film thickness), Absorbance spectra of $MAPbI_{3-x}Cl_x$ and $MAPbI_3$ reported devices, Photovoltaic characteristic curve and parameters of C343-DSC, cw-PIA in phase and out of phase signals, obtained with the same setup, for p-type device embedding $MAPbI_3$ perovskite. This material is available free of charge via the Internet at http://pubs.acs.org.

AUTHOR INFORMATION

Corresponding Author

*Phone: 0039-0832-1816241. E-mail: Andrea.Listorti@iit.it.

Notes

The authors declare no competing financial interest.

ACKNOWLEDGMENTS

This work was supported by EFOR (Iniziativa CNR per il Mezzogiorno L. 191/2009 art. 2 comma 44), by PON-MAAT (Project Number: PON02_00563_3316357 - CUP B31C12001230005), by PONFORM@BEYOND-NANO and by Regione PUGLIA (APQ Reti di Laboratorio, project "PHOEBUS" cod. 31). The authors gratefully acknowledge Dr. Alessandro Cannavale, Mrs. Sofia Masi, Mr. Valentino Pio Guerra, and Mr. Riccardo Scarfiello for fruitful discussions and technical support.

REFERENCES

(1) Lee, M. M.; Teuscher, J.; Miyasaka, T.; Murakami, T. N.; Snaith, H. J. Efficient Hybrid Solar Cells Based on Meso-Superstructured Organometal Halide Perovskites. *Science* **2012**, *338*, 643–647.

(2) Snaith, H. J. Perovskites: The Emergence of a New Era for Low-Cost, High- Efficiency Solar Cells. *J. Phys. Chem. Lett.* **2013**, *4*, 3623–3630.

(3) Grätzel, M. The Light and Shade of Perovskite Solar Cells. *Nat. Mater.* **2014**, *13*, 838–842.

(4) Green, M. A.; Ho-Baillie, A.; Snaith, H. J. The Emergence of Perovskite Solar Cells. *Nat. Photonics* **2014**, *8*, 506–514.

DOI: 10.1021/am508678p
ACS Appl. Mater. Interfaces 2015, 7, 4283–4289

(5) Park, N. Organometal Perovskite Light Absorbers Toward a 20% Efficiency Low-Cost Solid-State Mesoscopic Solar Cell. *J. Phys. Chem. Lett.* **2013**, *4*, 2423−2429.
(6) Stranks, S. D.; Eperon, G. E.; Grancini, G.; Menelaou, C.; Alcocer, M. J. P.; Leijtens, T.; Herz, L. M.; Petrozza, A.; Snaith, H. J. Electron-Hole Diffusion Lengths Exceeding 1 Micrometer in an Organometal Trihalide Perovskite Absorber. *Science* **2013**, *342*, 341−344.
(7) Wehrenfennig, C.; Eperon, G. E.; Johnston, M. B.; Snaith, H. J.; Herz, L. M. High Charge Carrier Mobilities and Lifetimes in Organolead Trihalide Perovskites. *Adv. Mater.* **2014**, *26*, 1584−1589.
(8) Deschler, F.; Price, M.; Pathak, S.; Klintberg, L. E.; Jarausch, D.-D.; Higler, R.; Hüttner, S.; Leijtens, T.; Stranks, S. D.; Snaith, H. J.; Atatüre, M.; Phillips, R. T.; Friend, R. H. High Photoluminescence Efficiency and Optically Pumped Lasing in Solution-Processed Mixed Halide Perovskite Semiconductors. *J. Phys. Chem. Lett.* **2014**, *5*, 1421−1426.
(9) Xing, G.; Mathews, N.; Sun, S.; Lim, S. S.; Lam, Y. M.; Gratzel, M.; Mhaisalkar, S.; Sum, T. C.; Grätzel, M. Long-Range Balanced Electron- and Hole-Transport Lengths in Organic-Inorganic CH3NH3PbI3. *Science* **2013**, *342*, 344−347.
(10) Wang, K.-C.; Jeng, J.-Y.; Shen, P.-S.; Chang, Y.-C.; Diau, E. W.-G.; Tsai, C.-H.; Chao, T.-Y.; Hsu, H.-C.; Lin, P.-Y.; Chen, P.; Guo, T.-F.; Wen, T.-C. P-Type Mesoscopic Nickel Oxide/organometallic Perovskite Heterojunction Solar Cells. *Sci. Rep.* **2014**, *4*, 4756.
(11) Roldán-Carmona, C.; Malinkiewicz, O.; Soriano, A.; Mínguez Espallargas, G.; Garcia, A.; Reinecke, P.; Kroyer, T.; Dar, M. I.; Nazeeruddin, M. K.; Bolink, H. J. Flexible High Efficiency Perovskite Solar Cells. *Energy Environ. Sci.* **2014**, *7*, 994−997.
(12) Eperon, G. E.; Burlakov, V. M.; Goriely, A.; Snaith, H. J. Neutral Color Semitransparent Microstructured Perovskite Solar Cells. *ACS Nano* **2014**, *8*, 591−598.
(13) Zhou, H.; Chen, Q.; Li, G.; Luo, S.; Song, T.-b.; Duan, H.-S.; Hong, Z.; You, J.; Liu, Y.; Yang, Y. Interface Engineering of Highly Efficient Perovskite Solar Cells. *Science* **2014**, *345*, 542−546.
(14) Ball, J. M.; Lee, M. M.; Hey, A.; Snaith, H. J. Low-Temperature Processed Mesosuperstructured to Thin-Film Perovskite Solar Cells. *Energy Environ. Sci.* **2013**, *6*, 1739−1743.
(15) Schulz, P.; Edri, E.; Kirmayer, S.; Hodes, G.; Cahen, D.; Kahn, A. Interface Energetics in Organo-Metal Halide Perovskite-Based Photovoltaic Cells. *Energy Environ. Sci.* **2014**, *7*, 1377−1381.
(16) Wang, J. T.-W.; Ball, J. M.; Barea, E. M.; Abate, A.; Alexander-Webber, J. A.; Huang, J.; Saliba, M.; Mora-Sero, I.; Bisquert, J.; Snaith, H. J.; Nicholas, R. J. Low-Temperature Processed Electron Collection Layers of graphene/TiO_2 Nanocomposites in Thin Film Perovskite Solar Cells. *Nano Lett.* **2014**, *14*, 724−730.
(17) Liu, D.; Kelly, T. L. Perovskite Solar Cells with a Planar Heterojunction Structure Prepared Using Room-Temperature Solution Processing Techniques. *Nat. Photonics* **2014**, *8*, 133−138.
(18) Heo, J. H.; Im, S. H.; Noh, J. H.; Mandal, T. N.; Lim, C.-S.; Chang, J. A.; Lee, Y. H.; Kim, H.; Sarkar, A.; Nazeeruddin, M. K.; Grätzel, M.; Seok, S. I. Efficient Inorganic−organic Hybrid Heterojunction Solar Cells Containing Perovskite Compound and Polymeric Hole Conductors. *Nat. Photonics* **2013**, *7*, 486−491.
(19) Liu, J.; Yongzhen, W.; Qin, C.; Yang, X.; Yasuda, T.; Islam, A.; Zhang, K.; Peng, W.; Han, L.; Chen, W. Dopant-Free Hole-Transporting Material for Efficient and Stable Perovskite Solar Cells. *Energy Environ. Sci.* **2014**, *7*, 2963−2967.
(20) Qin, P.; Tanaka, S.; Ito, S.; Tetreault, N.; Manabe, K.; Nishino, H.; Nazeeruddin, M. K.; Grätzel, M. Inorganic Hole Conductor-Based Lead Halide Perovskite Solar Cells with 12.4% Conversion Efficiency. *Nat. Commun.* **2014**, *5*, 3834.
(21) Docampo, P.; Ball, J. M.; Darwich, M.; Eperon, G. E.; Snaith, H. J. Efficient Organometal Trihalide Perovskite Planar-Heterojunction Solar Cells on Flexible Polymer Substrates. *Nat. Commun.* **2013**, *4*, 2761.
(22) Jeng, J.-Y.; Chen, K.-C.; Chiang, T.-Y.; Lin, P.-Y.; Tsai, T.-D.; Chang, Y.-C.; Guo, T.-F.; Chen, P.; Wen, T.-C.; Hsu, Y.-J. Nickel Oxide Electrode Interlayer in CH3 NH3 PbI3 Perovskite/PCBM Planar-Heterojunction Hybrid Solar Cells. *Adv. Mater.* **2014**, *26*, 4107−4113.
(23) Seo, J.; Park, S.; Chan Kim, Y.; Jeon, N. J.; Noh, J. H.; Yoon, S. C.; Seok, S. Il. Benefits of Very Thin PCBM and LiF Layers for Solution-Processed P−i−n Perovskite Solar Cells. *Energy Environ. Sci.* **2014**, *7*, 2642−2646.
(24) Krebs, F. C.; Tromholt, T.; Jørgensen, M. Upscaling of Polymer Solar Cell Fabrication Using Full Roll-to-Roll Processing. *Nanoscale* **2010**, *2*, 873−886.
(25) D'Innocenzo, V.; Grancini, G.; Alcocer, M. J. P.; Kandada, A. R. S.; Stranks, S. D.; Lee, M. M.; Lanzani, G.; Snaith, H. J.; Petrozza, A. Excitons versus Free Charges in Organo-Lead Tri-Halide Perovskites. *Nat. Commun.* **2014**, *5*, 3586.
(26) Roiati, V.; Colella, S.; Lerario, G.; Marco, L.; De Rizzo, A.; Listorti, A.; Gigli, G. Investigating Charge Dynamics in Halide Perovskitesensitized Mesostructured Solar Cells. *Energy Environ. Sci.* **2014**, *7*, 1889−1894.
(27) Kim, H.-S.; Mora-Sero, I.; Gonzalez-Pedro, V.; Fabregat-Santiago, F.; Juarez-Perez, E. J.; Park, N.-G.; Bisquert, J. Mechanism of Carrier Accumulation in Perovskite Thin-Absorber Solar Cells. *Nat. Commun.* **2013**, *4*, 2242.
(28) Gonzalez-Pedro, V.; Juárez-Pérez, E. J.; Arsyad, W. S.; Barea, M.; Fabregat-Santiago, F.; Mora-Sero, I.; Bisquert, J. General Working Principles of CH 3 NH 3 PbX 3 Perovskite Solar Cells. *Nano Lett.* **2014**, *14*, 888−893.
(29) Edri, E.; Kirmayer, S.; Henning, A.; Mukhopadhyay, S.; Gartsman, K.; Rosenwaks, Y.; Hodes, G.; Cahen, D. Why Lead Methylammonium Tri-Iodide Perovskite-Based Solar Cells Require a Mesoporous Electron Transporting Scaffold (but Not Necessarily a Hole Conductor). *Nano Lett.* **2014**, *14*, 1000−1004.
(30) Edri, E.; Kirmayer, S.; Mukhopadhyay, S.; Gartsman, K.; Hodes, G.; Cahen, D. Elucidating the Charge Carrier Separation and Working Mechanism of CH3NH3PbI(3-x)Cl(x) Perovskite Solar Cells. *Nat. Commun.* **2014**, *5*, 3461.
(31) Dualeh, A.; Moehl, T.; Tetreault, N.; Teuscher, J.; Gao, P.; Nazeeruddin, M. K.; Gratzel, M. Impedance Spectroscopic Analysis of Lead Iodide Perovskite-Sensitized Solid-State Solar Cells. *ACS Nano* **2014**, *8*, 362−373.
(32) Laban, W. A.; Etgar, L. Depleted Hole Conductor-Free Lead Halide Iodide Heterojunction Solar Cells. *Energy Environ. Sci.* **2013**, *6*, 3249−3253.
(33) Snaith, H. J.; Abate, A.; Ball, J. M.; Eperon, G. E.; Leijtens, T.; Noel, N. K.; Stranks, S. D.; Wang, J. T.-W.; Wojciechowski, K.; Zhang, W. Anomalous Hysteresis in Perovskite Solar Cells. *J. Phys. Chem. Lett.* **2014**, *5*, 1511−1515.
(34) Unger, E. L.; Hoke, E. T.; Bailie, C. D.; Nguyen, W. H.; Bowring, A. R.; Heumuller, T.; Christoforo, M. G.; McGehee, M. D. Hysteresis and Transient Behavior in Current-Voltage Measurements of Hybrid-Perovskite Absorber Solar Cells. *Energy Environ. Sci.* **2014**, *7*, 3690−3698.
(35) Wang, K.; Shen, P.; Li, M.; Chen, S.; Lin, M.; Chen, P.; Guo, T. Low-Temperature Sputtered Nickel Oxide Compact Thin Film as Effective Electron Blocking Layer for Mesoscopic NiO/CH3NH3PbI3 Perovskite Heterojunction Solar Cells. *ACS Appl. Mater. Interfaces* **2014**, *6*, 11851−11858.
(36) Zhu, Z.; Bai, Y.; Zhang, T.; Liu, Z.; Long, X.; Wei, Z.; Wang, Z.; Zhang, L.; Wang, J.; Yan, F.; Yang, S. High-Performance Hole-Extraction Layer of Sol-Gel-Processed NiO Nanocrystals for Inverted Planar Perovskite Solar Cells. *Angew. Chem., Int. Ed.* **2014**, *53*, 12571−12575.
(37) Ma, W.; Song, H.; Chen, W.; Cheng, Y.; Tang, J. Sequential Deposition of $CH_3NH3PbI_3$ on Planar NiO Film for Efficient Planar Perovskite Solar Cells. *ACS Photonics* **2014**, *1*, 547−553.
(38) Wang, K.; Shen, P.; Li, M.; Chen, S.; Lin, M.; Chen, P.; Guo, T. Low-Temperature Sputtered Nickel Oxide Compact Thin Film as Effective Electron Blocking Layer for Mesoscopic NiO/CH3NH3PbI3 Perovskite Heterojunction Solar Cells. *ACS Appl. Mater. Interfaces* **2014**, *6*, 11851−11858.

DOI: 10.1021/am508678p
ACS Appl. Mater. Interfaces 2015, 7, 4283−4289

(39) Sarkar, S. K.; Subbiah, A. S.; Halder, A.; Ghosh, S.; Mahuli, N.; Hodes, G. Inorganic Hole Conducting Layers for Perovskite-Based Solar Cells. *J. Phys. Chem. Lett.* **2014**, *5*, 1748−1753.
(40) Roiati, V.; Mosconi, E.; Listorti, A.; Colella, S.; Gigli, G.; De Angelis, F. Stark Effect in Perovskite/TiO2 Solar Cells: Evidence of Local Interfacial Order. *Nano Lett.* **2014**, *14*, 2168−2174.
(41) De Bastiani, M.; D'Innocenzo, V.; Stranks, S. D.; Snaith, H. J.; Petrozza, A. Role of the Crystallization Substrate on the Photoluminescence Properties of Organo-Lead Mixed Halides Perovskites. *APL Mater.* **2014**, *2*, 081509.
(42) Leijtens, T.; Stranks, S. D.; Eperon, G. E.; Lindblad, R.; Johansson, E. M. J.; McPherson, I. J.; Rensmo, H.; Ball, J. M.; Lee, M. M.; Snaith, H. J. Electronic Properties of Meso-Superstructured and Planar Organometal Halide Perovskite Films: Charge Trapping, Photodoping, and Carrier Mobility. *ACS Nano* **2014**, *8*, 7147−7155.
(43) Mizoguchi, Y.; Fujihara, S. Fabrication and Dye-Sensitized Solar Cell Performance of Nanostructured NiO/Coumarin 343 Photocathodes. *Electrochem. Solid-State Lett.* **2008**, *11*, K78−K80.
(44) Zhu, H.; Hagfeldt, A.; Boschloo, G. Photoelectrochemistry of Mesoporous NiO Electrodes in Iodide/Triiodide Electrolytes. *J. Phys. Chem. C* **2007**, *111*, 17455−17458.
(45) Boschloo, G.; Hagfeldt, A. Photoinduced Absorption Spectroscopy of Dye-Sensitized Nanostructured TiO2. *Chem. Phys. Lett.* **2003**, *370*, 381−386.
(46) Morandeira, A.; Boschloo, G.; Hagfeldt, A.; Hammarstro, L. Coumarin 343 - NiO Films as Nanostructured Photocathodes in Dye-Sensitized Solar Cells: Ultrafast Electron Transfer, Effect of the I 3-/I- Redox Couple and Mechanism of Photocurrent Generation. *J. Phys. Chem. C* **2008**, *112*, 9530−9537.
(47) Gégout, A.; Delgado, J. L.; Nierengarten, J.-F.; Delavaux-Nicot, B.; Listorti, A.; Chiorboli, C.; Belbakra, A.; Armaroli, N. Photoinduced Electron Transfer in a Fullerene−oligophenylenevinylene Dyad. *New J. Chem.* **2009**, *33*, 2174−2182.
(48) Lee, J.-W.; Seol, D.-J.; Cho, A.-N.; Park, N.-G. High-Efficiency Perovskite Solar Cells Based on the Black Polymorph of HC(NH2)2 PbI3. *Adv. Mater.* **2014**, *26*, 4991−8.
(49) Chen W.; Wu Y.; Liu J.; Qin C.; Yang X.; Islam A.; Cheng Y. B.; Han L. Hybrid interfacial layer leads to solid performance improvement of inverted perovskite solar cells. *Energy Environ. Sci.* **2015**, Advance Article DOI: 10.1039/C4EE02833C.

DOI: 10.1021/am508678p
ACS Appl. Mater. Interfaces 2015, 7, 4283−4289